

An investigation of the free surface effect

Nasser S. Hamarbitan and Gary F. Margrave,

ABSTRACT

When P and S seismic waves are incident on a solid-air interface at a non-normal angle, the displacement of each wave will be observed on both vertical and horizontal geophones at the interface. Since the incident waves will cause P and S reflections (the free surface effect), and since the geophones record the total displacement at the interface due to all waves, a complete understanding must consider not just the emergence angle but also the resulting reflections.

Simple considerations for body waves predict a particle displacement vector which points in the direction of propagation for P waves, and perpendicular to it for S waves. The effect of the free surface is to cause the displacement vector for P waves to deflect towards the vertical and towards the horizontal for S waves.

We derived a theoretical expression from the Zoeppritz equations, which relates the emergence and displacement angles as a function of V_p/V_s . Then a Matlab program was built to study the relationship between the particle displacement angle and emergence angle for selected events in a seismic shot record. Given the (t,x) description for the trajectory of an event, the program models by least squares each component of displacement and the wavefront shape as low order polynomials in offset. The polynomials of the displacement component were used to estimate the direction of the displacement vector and the wavefront shape polynomial together with a value for the weathering velocity, was used to estimate the emergence angle.

This method was applied on a shot record from the Blackfoot broad-band survey and we observed that there are many effects in real data which complicate these measurements including interfering wavetypes, near surface material variations, static anomalies, and random noise. Nevertheless our results are broadly consistent with free surface theory and suggest V_p/V_s ratios in the range of 5 or greater will characterize the Blackfoot weathering layer.

INTRODUCTION

In 3-c shot records, we can recognize different types of events: refractions, surface waves and shear waves along with P waves. These waves are recorded in their true amplitude. In general we can not see shear waves as clearly as P waves because the frequency band is smaller for S waves and they are attenuated more strongly in the near surface.

Current methods of P and S wave separation are based on the work of Dankbaar (1985) who showed how to use the free surface theory to design a linear mode separation (or modal filter). Later Donati and Stewart (1994) showed the P-S separation filter in the tau-p domain worked well on synthetic data and was effective in eliminating noise like ground-roll.

These methods work very well on synthetic data but are troubled by noise and interfering wavetypes on real data. In order to better understand the physical effects which determine the frequency band of S waves and to estimate the V_p/V_s ratio in the near surface, we investigate the theory of the free surface effect and compare it with

measurements from real data of the emergence and displacement angles. We hope to be able to define the type of recorded wave for any event in a source record.

THEORY

Defining the wave type in a shot record is based on the value of the displacement angle (ϕ) in relation to emergent angle(θ). For P waves, propagation is in the direction of the particle displacement, while for S waves the propagation is perpendicular to it. From these concepts, our measurements and analysis are based on computing the total displacement vector, the displacement angle and the emergent angle using the weathering velocity information which we obtained from the Blackfoot survey.

A) Measurement

Let x denote the inline direction of a 2-D, 3-C shot record and y the crossline direction. Then we define $\theta(x,y,t)$ as the emergent angle of the seismic wavefront recorded on the 3-C record at (x,y,t) (figure 1). We also define $\phi(x,y,t)$ as the angle defined by the 3-C particle displacement vector recorded in the geophone. (Both angles are defined with respect to the positive x axis.)

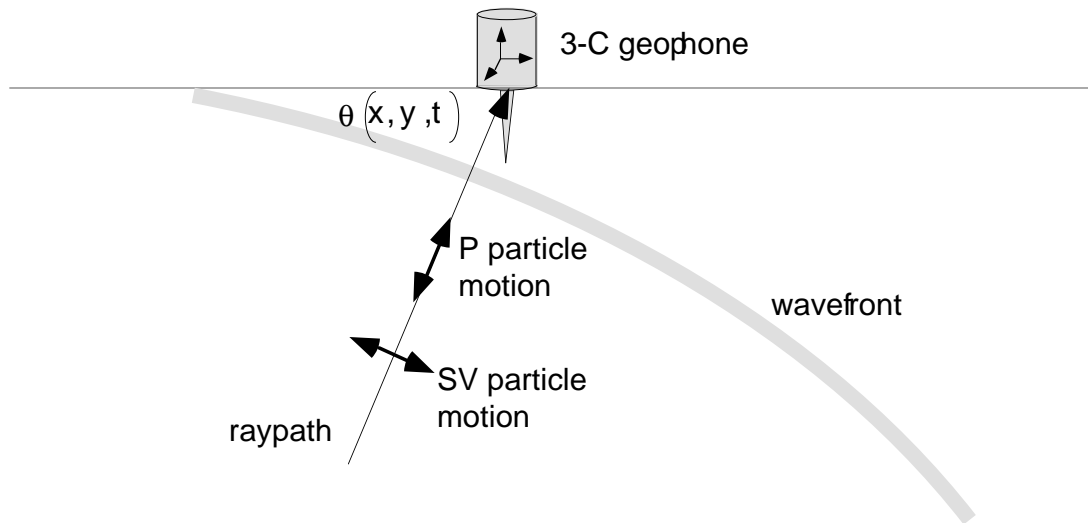


FIG. 1. A wavefront with emergent angle $\theta(x,y,t)$ is recorded by a 3-C geophone.

If the components of displacement are (u_x, u_y, u_z) , then the particle displacement angle can be found from:

$$\sin(\phi) = \frac{u_x}{|\vec{u}|} \quad (1a)$$

or alternatively, for radial and vertical components (u_r, u_v)

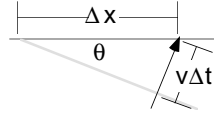
$$\tan(\phi) = \frac{u_r}{u_v} \quad (1b)$$

where

$$|\vec{u}| = \sqrt{u_x^2 + u_y^2 + u_z^2} \quad (2)$$

If a particular event on the seismogram is "picked", its apparent velocity, v_a , can be used to compute $\theta(x,y,t)$ as follows:

$$\sin(\theta) = \frac{v\Delta t}{\Delta x} = \frac{v}{v_a} \quad (3)$$



where

$$v_a = \frac{\Delta x}{\Delta t} \quad (4)$$

Note that eqn (1) determines an angle in 3-D while, given a 2-D seismic record, eqn (3) determines an angle in the (x,z) plane. However, for a stratified medium it can be shown that P-SV motion is decoupled from SH and that SV waves are characterized by particle motion in the (x,z) plane. Thus we expect that a statistically non-zero u_y will be the exceptional case.

As defined by equation (3) the emergence angle is computed across a span of traces, Δx , in width while the particle displacement angle, as defined by (1), can be computed for a single trace. The complex interference of various wave types on a seismic record generally causes displacement angles to differ from the simple theoretical expectations. It is expected that the computation of some kind of "average" angle for the displacement vector across the same trace ensemble used to compute the emergence angle will give improved results.

B) Analysis

Since P waves are characterized by particle motion in the direction of wave propagation we expect:

$$\theta = \phi \text{ for P waves} \quad (5)$$

Conversely, for S waves the particle motion is at right angle to the propagation direction so the expectation is:

$$\theta = \phi \pm 90^\circ \text{ for SV waves} \quad (6)$$

We can compute a scalar quantity which is a measure of whether a wave is P or S as:

$$PS = \cos(\theta - \phi) \quad (7)$$

We see that PS is exactly 1 for a P wave and 0 for an SV wave.

Note that the computation of the emergence angle θ requires a velocity which is assumed to be the near surface velocity for P or S waves as appropriate. Since we do not know the wave type, apriori, the computation of PS must be done twice using both

v_p and v_s and the results interpreted. We also note that for a given picked event and corresponding apparent velocity, only subsurface velocities not larger than v_a will result in real emergence angles. It also seems possible to turn this method around and, by picking "known" P or S events, compute v_p and v_s .

Equations (5), (6), and (7) are probably unrealistic since they do not recognize that the 3-C recording takes place on a *free surface*. Dankbaar (1985) gives expressions for the expected horizontal and vertical component receiver measurements assuming an incident P or SV wave on a free surface. These expressions are derivable from the Zoeppritz equations (Aki and Richards 1980) and predict considerable departure from the simple body wave expectations outline above. Assuming an incident P wave, Dankbaar's expressions lead to the following relationship between θ and ϕ :

$$\tan(\phi) = \frac{2\sin(\theta)\sqrt{r^2 - \sin^2(\theta)}}{r^2 - 2\sin^2(\theta)} \text{ for P waves} \quad (8)$$

while the S wave expression is:

$$\tan(\phi) = \frac{r(1 - 2\sin^2(\theta))}{2\sin(\theta)\sqrt{1 - r^2\sin^2(\theta)}} \text{ for S waves} \quad (9)$$

in both of these expressions:

$$r = \frac{v_p}{v_s} \quad (10)$$

For an assumed $r = 2$, figure 2 graphs equations (8) and (9).

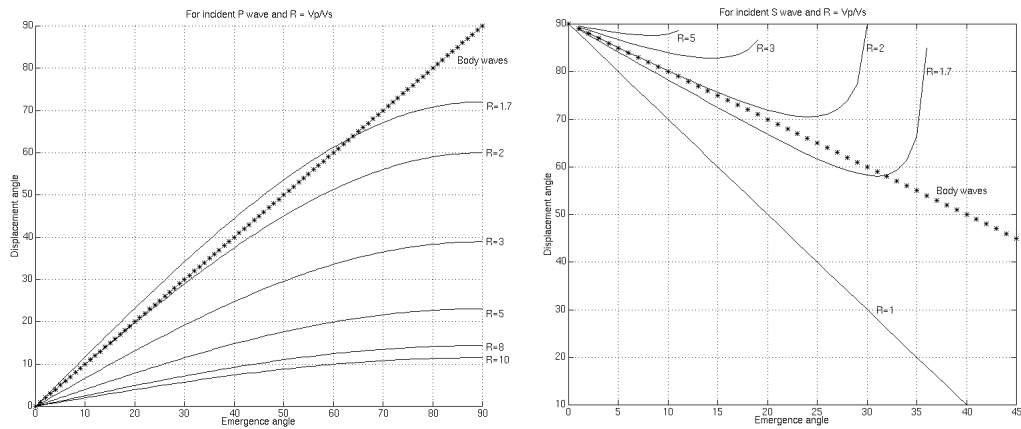


FIG. 2. On the left is a plot of equation (8) for $r = 2$, while equation (9) is shown on the right for the same circumstance.

It can be concluded from this brief investigation of the free surface effect that for emergence angles near vertical both P and S waves show approximately the same relation between θ and ϕ as that expected for body waves. As emergence angles exceed 20 degrees, significant new behavior arises though there is still good reason to believe

that computation of the PS scalar with equation (7) will distinguish between the wave types.

METHOD

We have developed a numerical analysis method to study the applicability of free surface theory to a real exploration setting. In essence, we pick events on one component or another, determine their amplitudes on all components, and estimate the direction of the displacement vector. The trajectory of the event is then used to estimate the emergence angle. We hope that by studying the relationship between these angles, we can determine the nature of the event.

The method is based on choosing some events to characterize the reflections and refractions. The following procedures were implemented in a Matlab program.

- An event is picked (graphically) on either the vertical or radial component. The picked component is designated as the “primary component”.
- The picks are adjusted to the nearest peak on the primary component.
- The amplitude variation with offset was modeled as a low order polynomial for each component. We used polynomial order of 2 for the primary component and 1 for the secondary component.
- The displacement vector angle, ϕ , was then computed as the arctangent of the ratio of the fitted radial amplitudes divided by the fitted vertical .
- The adjusted pick times are also fitted with a second order polynomial in offset. The average emergence angle was then computed using an assumed weathering velocity.

APPLICATION AND RESULTS.

In this study four strong events in both vertical and radial components were picked to characterize reflection and refraction events. A given event is generally more apparent on one component than the other. The component on which it is more visible is called the primary component. The estimation of emergence angle requires a weathering velocity estimate. Except where otherwise noted, we used 1000 m/sec for P waves (suggested by uphole information) and 500 m/sec for S waves, As will be seen, the later figure is probably too large.

The data used for this study came from the Blackfoot broad-band survey using 10 hz 3C geophones. A surface consistent amplitude adjustment was performed in Promax to compensate for variations in geophone to surface coupling. Otherwise the data is raw.

Event #1 was picked from the vertical component, which is therefore primary (figure 3). The same (t,x) description for this event was plotted on the radial component. Note that this event is obvious in the vertical component but hardly discernible on the radial component. The low amplitude of the event on the radial component and strong interference of other wave types makes these measurements difficult.

Figure 4 shows the raw vertical and radial amplitudes (AVRAW and ARRAW) and their resultant polynomial fits (AV and AR) as computed by our algorithm. From this figure we can say it is more likely that this event is a P wave reflection as the average

vertical amplitude (AV) ranges from 10 to 30, while the radial amplitude (AR) is almost zero for the whole event.

To support the previous assumption, figure 5 shows the emergent and displacement angles as functions of offset. Both theta and phi have almost the same values against each point in the offset axis. This agrees with the theory of P wave behavior which indicates that the direction of the particle displacement is always in the direction of the propagation.

Figure 6a shows the relation between theta and phi for the same event. Comparing this with figure 2 (left) shows very rough qualitative agreement with P wave behavior but it is difficult to say more. In figure 6b we show event #1 for two different weathering velocities as well as several of the theoretical curves. The weathering velocity of 1000 m/s is consistent with measured uphole times of Blackfoot survey while 2000 m/s is more consistent with the near offset first arrivals. The curvature of the two curves for event #1 is probably an artifact of our method and represents the uncertainty in V_p/V_s estimates. Nevertheless we feel that V_p/V_s is much greater than 2 and probably greater than 5 in the near surface.

Event #2 was a possible S wave reflection and was picked on the radial component (figure 7). An indication of the wavetype from figure 8 is that the amplitude of this event is ranging from -1 to 2 in the vertical component and from 1 to 8 in the radial component. This is a strong suggestion of an S wave reflection; however, much of the variability in these amplitudes is probably from interfering P waves.

Figure 9 shows the fitted vertical and radial displacements plotted versus offset and figure 10 shows theta plotted versus phi and is quite distinct in character from figure 6a. Thus it is likely that event #1 and event #2 are different wavetypes, therefore event #2 is likely an S wave reflection. When compared with figure 2 (right) we again see broad similarities but differences in detail. However the overall suggestion is clearly an S wave since the angles are mostly orthogonal.

Event #3 was picked to characterize a likely P wave refraction in the near surface as is shown in figures 11. It is very strong on the vertical component but weaker on the radial and much noisier. As we can see from figure 12, the amplitude of the event is in the range of 50 to 120 in the vertical component and it is 5 to 7 in the radial component. This is a good indication of a P wave.

Figures 13 and 14 suggest that the event is more likely a P wave than an S wave because the angles are fairly similar. Furthermore; noting that theta is nearly constant (as would be expected for a refraction) at 20 degrees and comparing with figure 2 (left) we see that a V_p/V_s ratio of 5 or greater is again indicated.

Event #4 is similar to event #3 as both characterize refractions; however, we expect this is an S wave refraction. Figure 15 shows the event on the vertical and radial components. Analyzing figure 16, we can see that the overall power level on the radial component is about 20 times greater than on the vertical component. This difference strongly suggestive of an S wave.

As we can see from figure 17, there is a difference of 70 degrees between theta and phi. An S wave refraction should have a difference of nearly 90 degrees while a difference close to zero degrees would indicate P wave refraction. The difference of 70 degrees suggests that this refracted event is an S wave.

As with P wave refraction, we see that this event has a constant emergence angle of about 20 degrees (assuming a shear wave weathering velocity of 500 m/sec). Comparing with figure 2 (right) we see that a V_p/V_s ratio of between 2 and 3 is indicated. However; if the P wave analyses are to be believed, then V_p/V_s is more likely near 5. This would require an S wave weathering velocity of 200 m/sec which would lower theta (figure 17) to 10 degrees or less. Comparing again with figure 2 (right), results consistent with the P wave refraction can be obtained for V_p/V_s of about 5. Theta is shown versus phi for event 4 in figure 18.

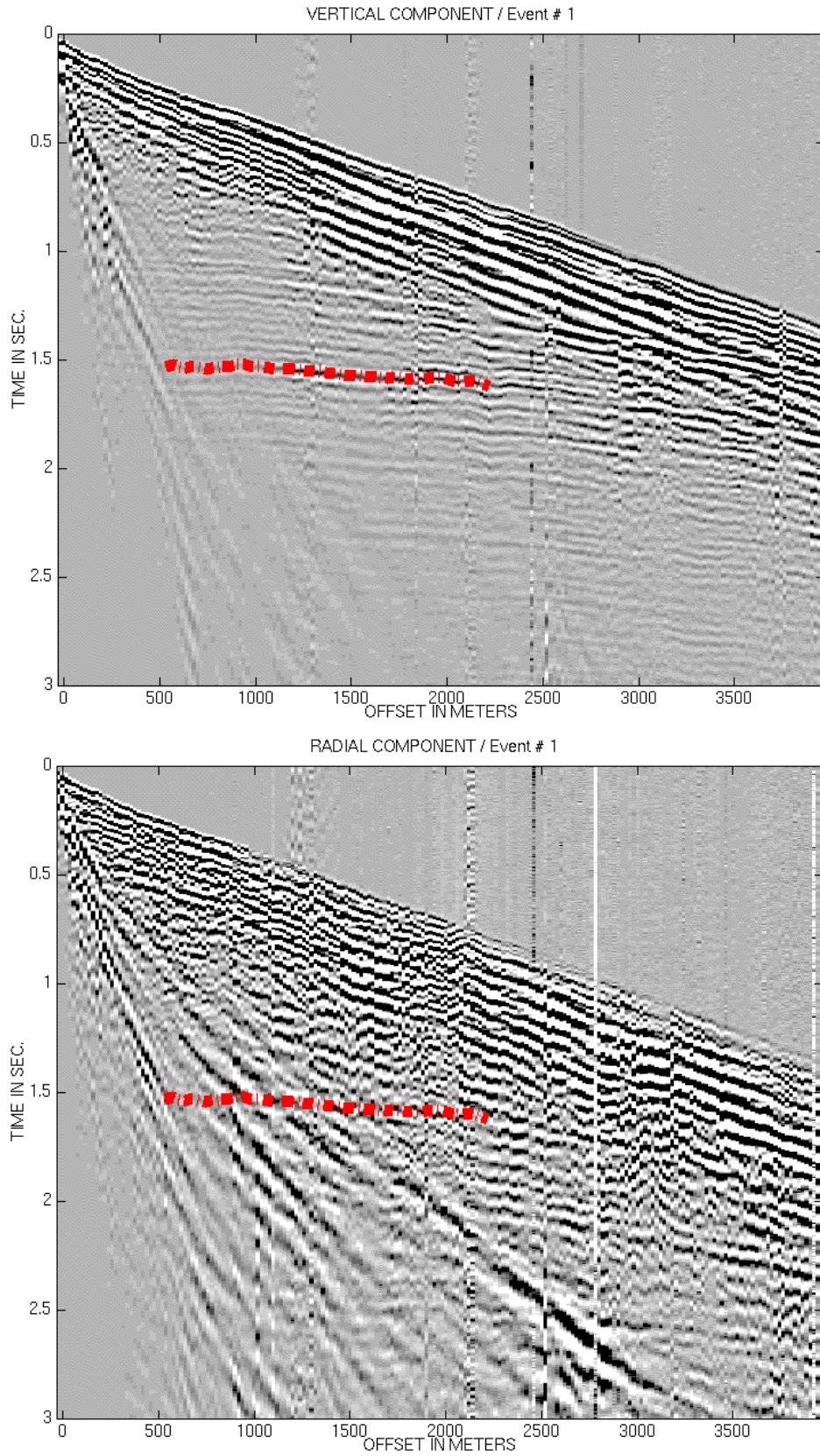


FIG. 3. Event # 1 on the vertical and radial components.

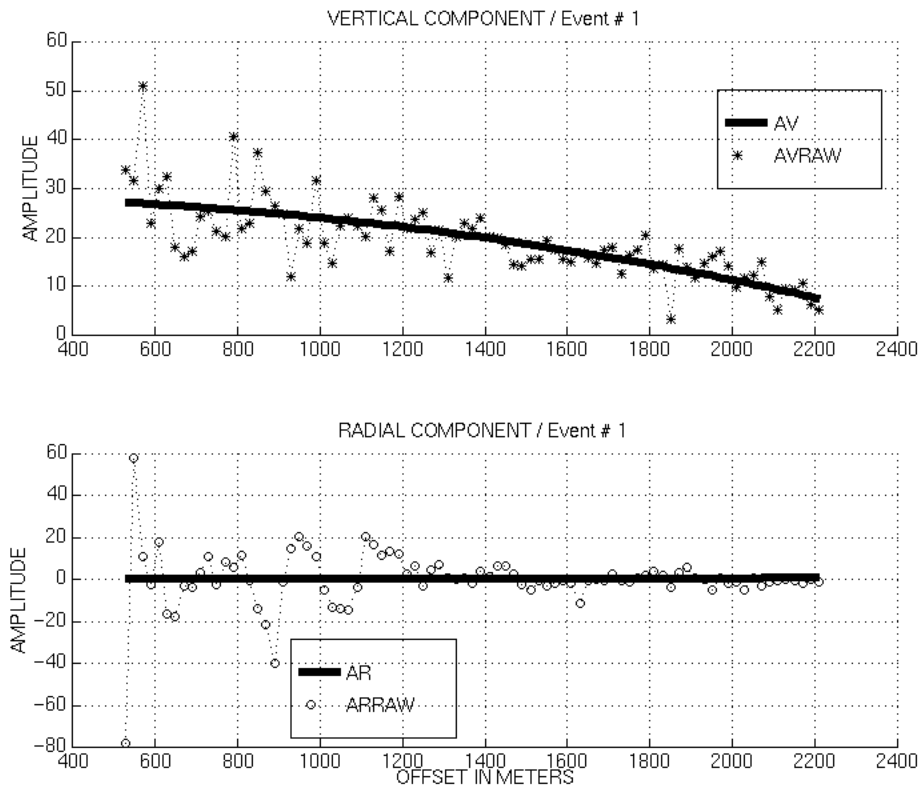


FIG. 4. The amplitudes of the vertical and radial components (AVRAW,ARRAW) and their polynomial fits (AV,AR) for event #1.

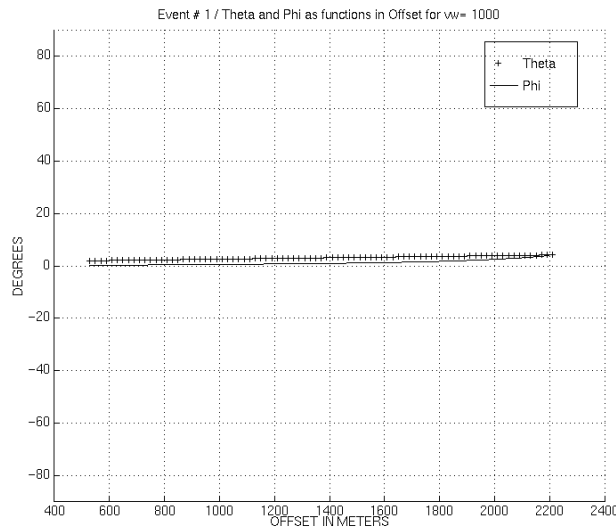


FIG.5. The emergence and displacement angles as functions of offset for event #1.

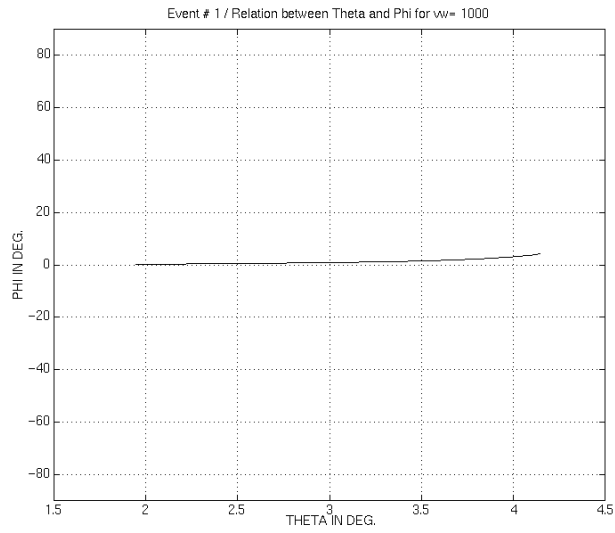


FIG. 6a. The relation between the emergence angle (theta) and the displacement angle (phi)

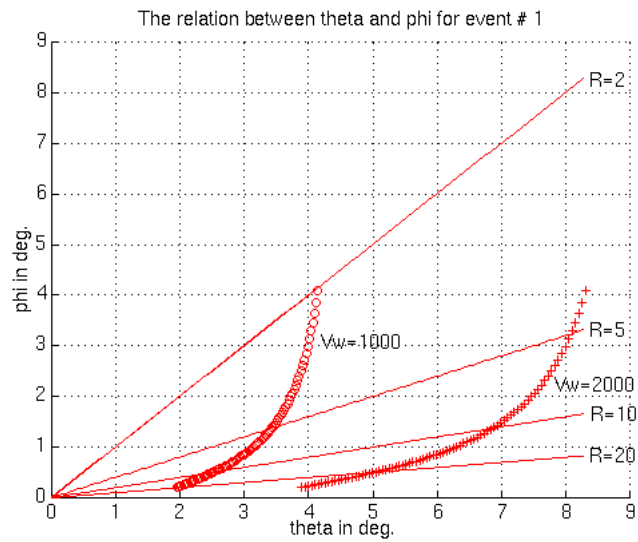


FIG. 6b. The relation between theta and phi for event #1 compared with theoretical prediction for different V_p/V_s values ($V_p/V_s=R$).

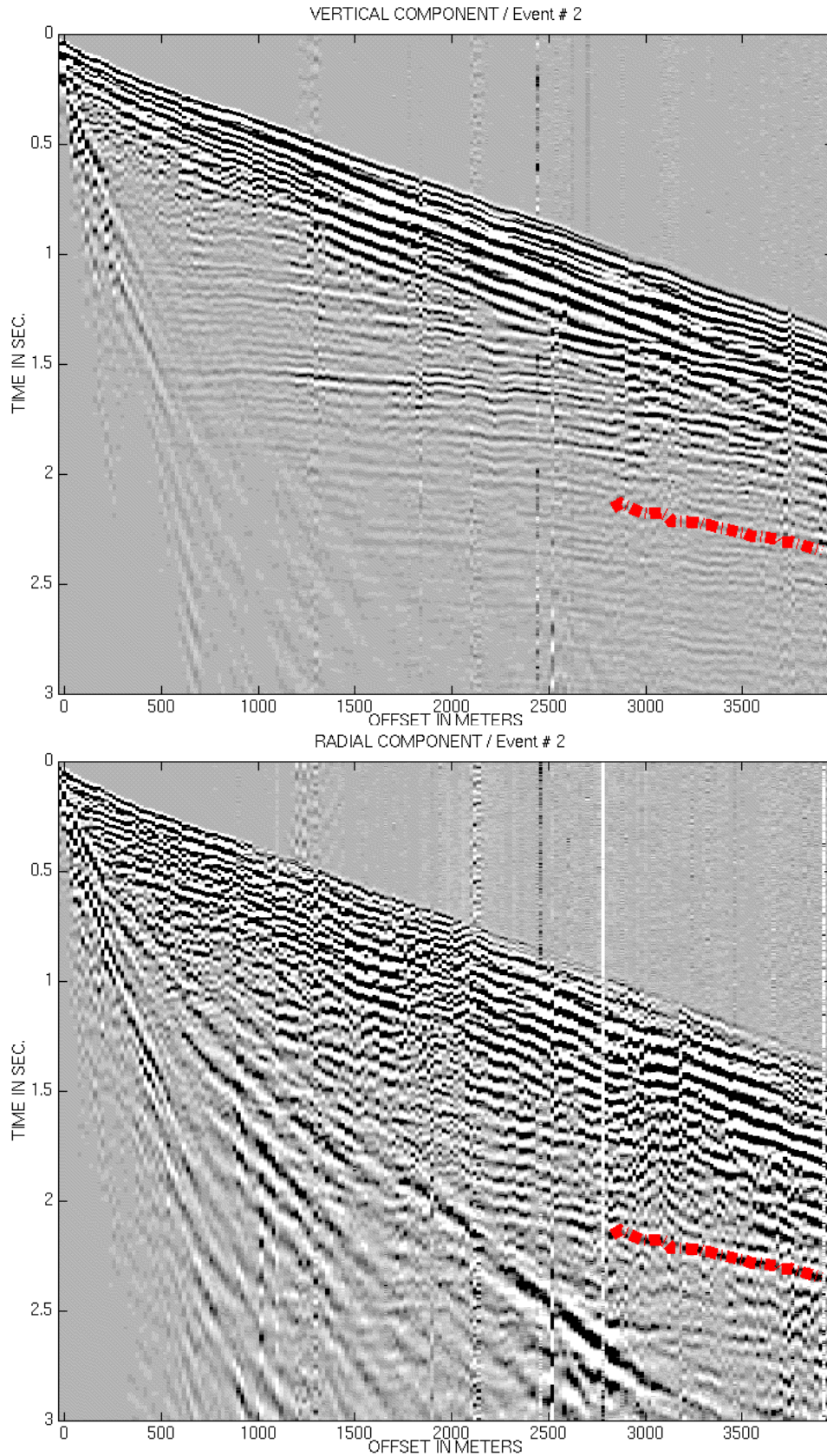


FIG. 7. Event #2 on the vertical and radial components.

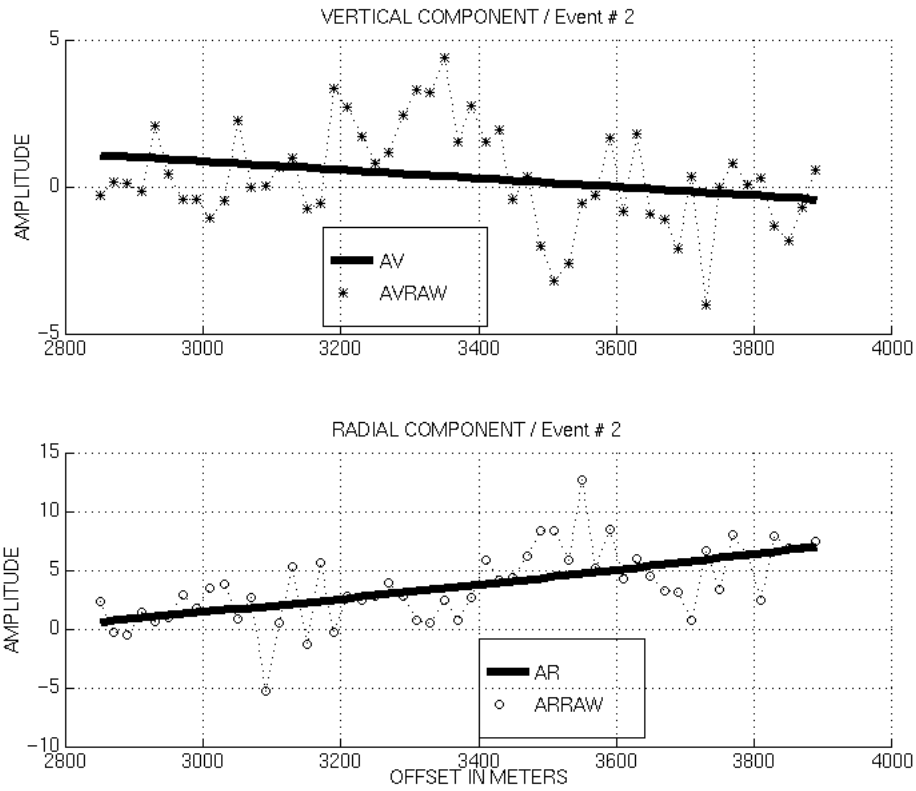


FIG. 8. The amplitudes of the vertical and radial components (AVRAW,ARRAW) and their fitted polynomials (AV,AR).

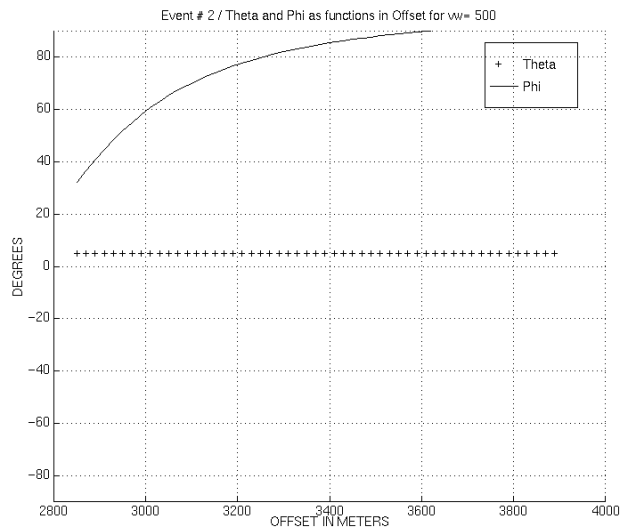


FIG. 9. The emergence and displacement angles as functions of offset for event #2.

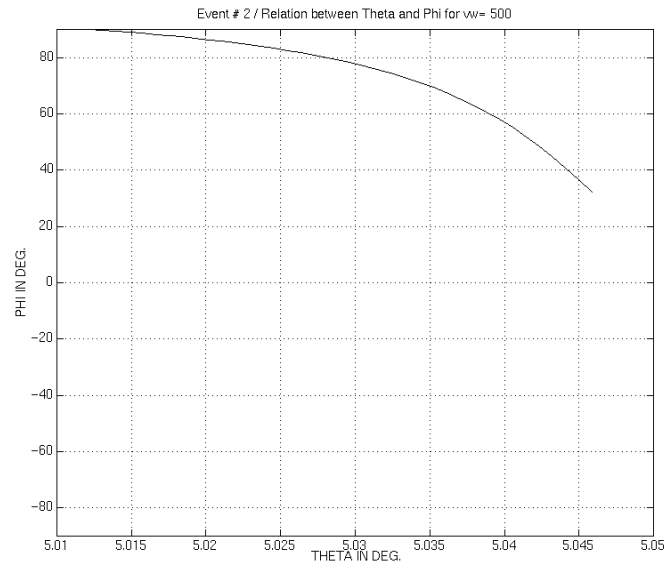


FIG. 10. The relation between theta and phi for event #2.

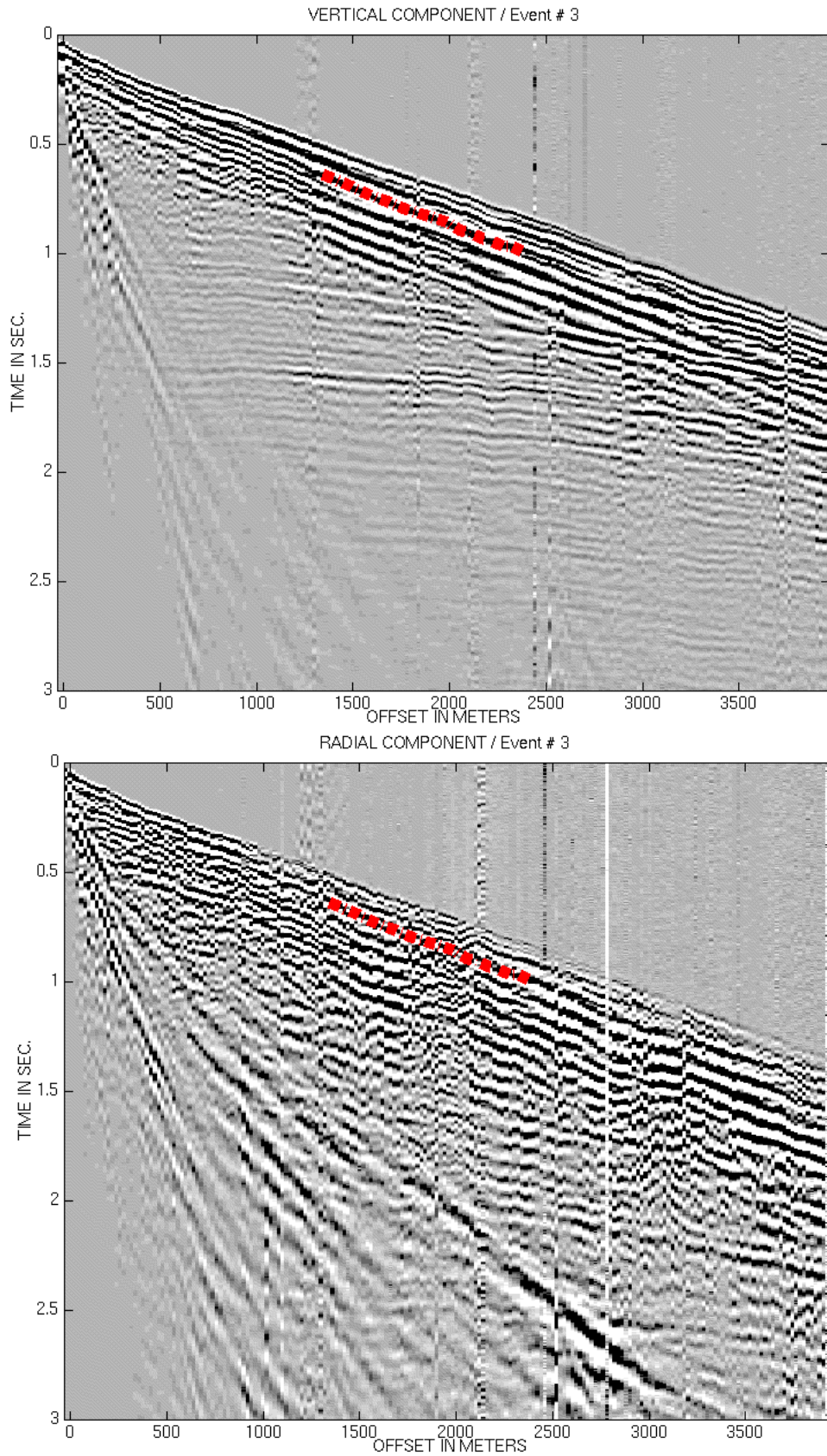


FIG. 11. Event #3 in the vertical and radial components.

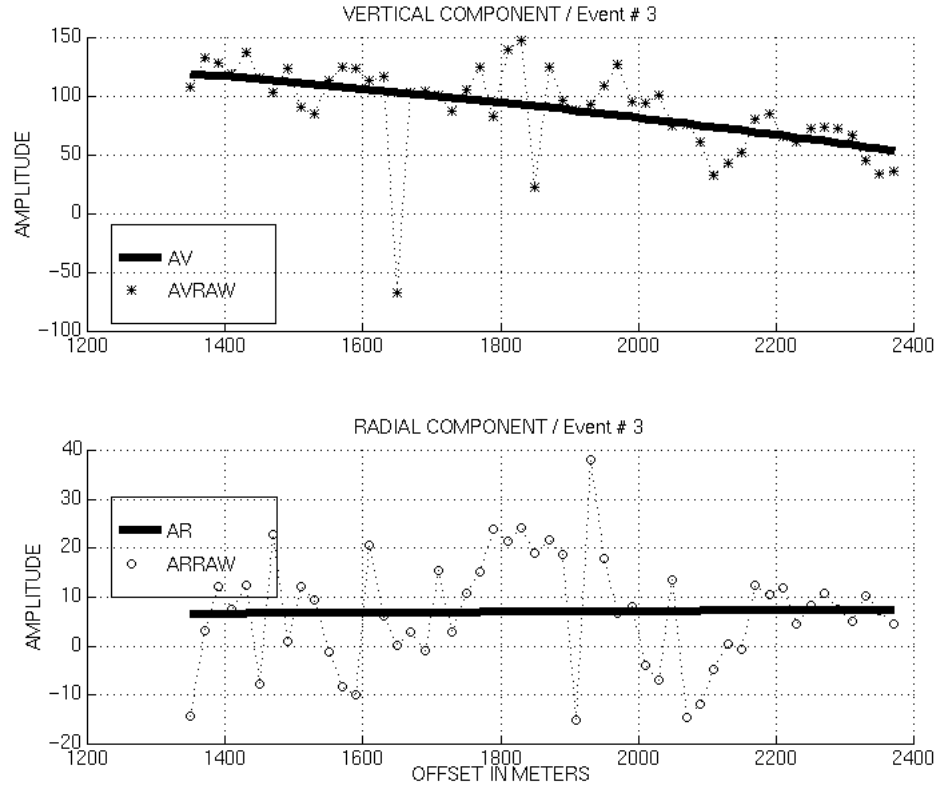


FIG. 12. The amplitudes of the vertical and radial components(AVRAW,ARRAW) and their polynomial fits(AV,AR) for event #3.

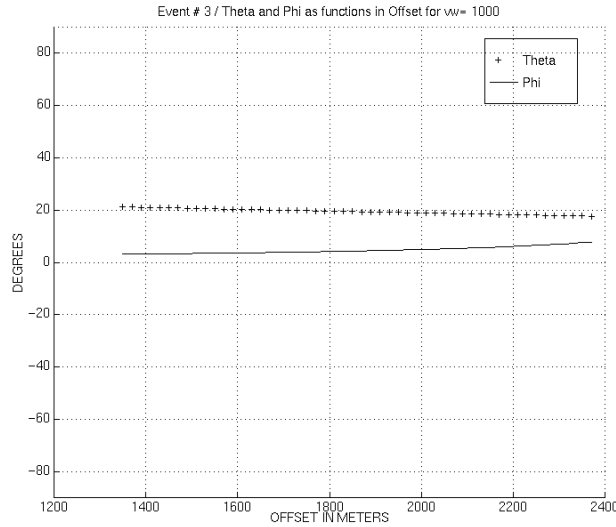


FIG. 13. The emergent angle (theta) and displacement angle (phi) as functions of offset.

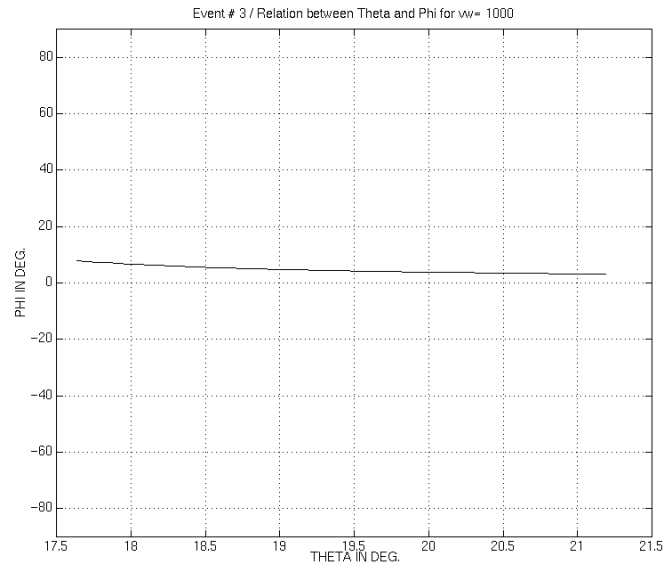


FIG. 14. The relation between theta and phi for event #3.

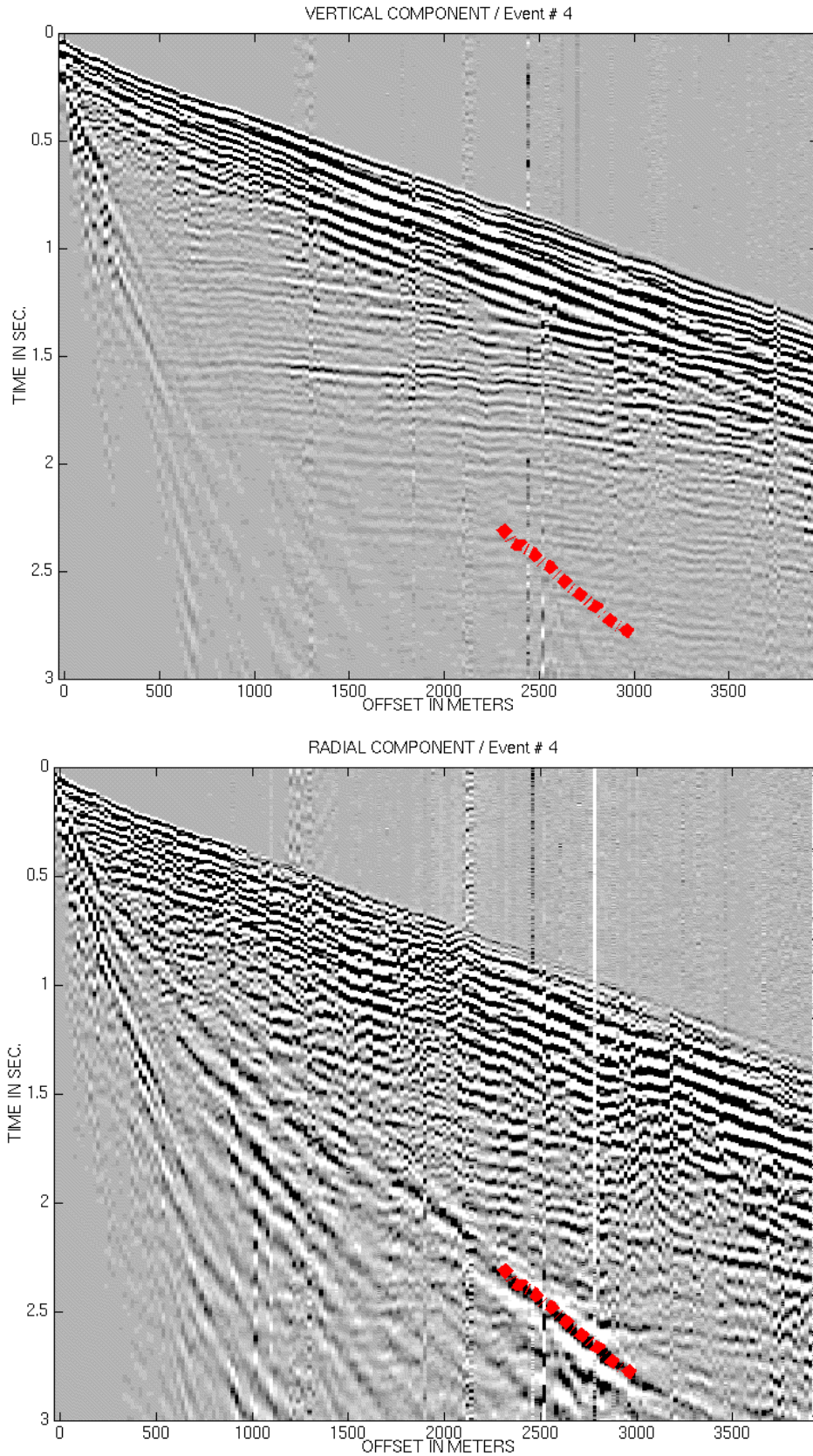


FIG. 15. Event #4 in the vertical and radial components.

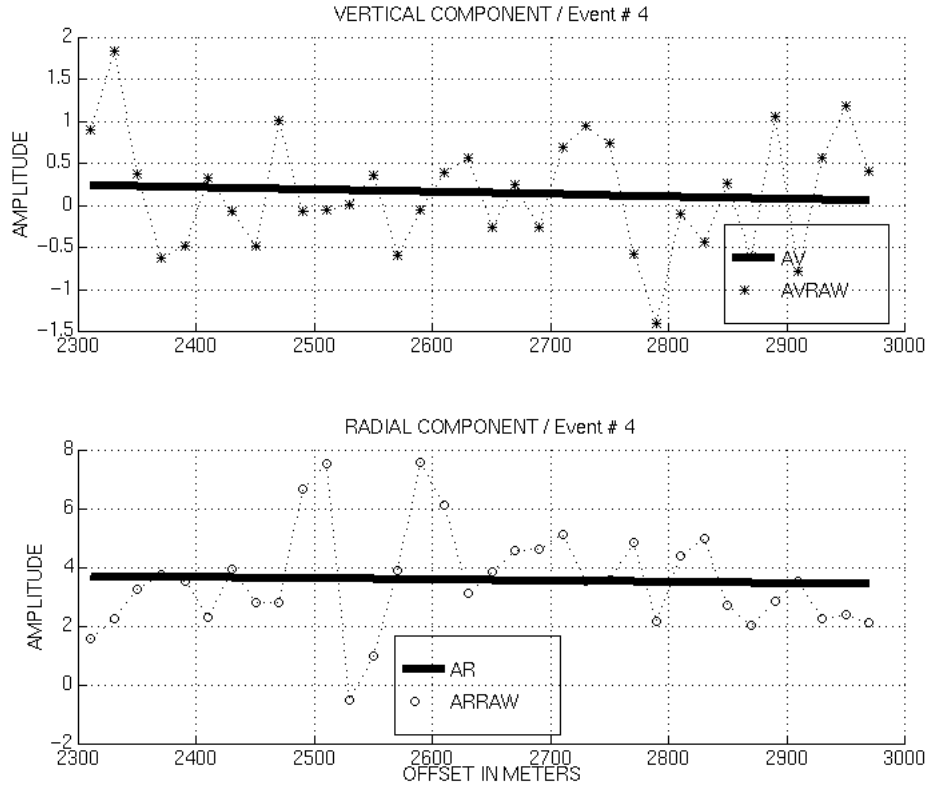


FIG.16. The amplitudes of the vertical and radial components(AVRAW,ARRAW) and their fitted polynomials(AV,AR).

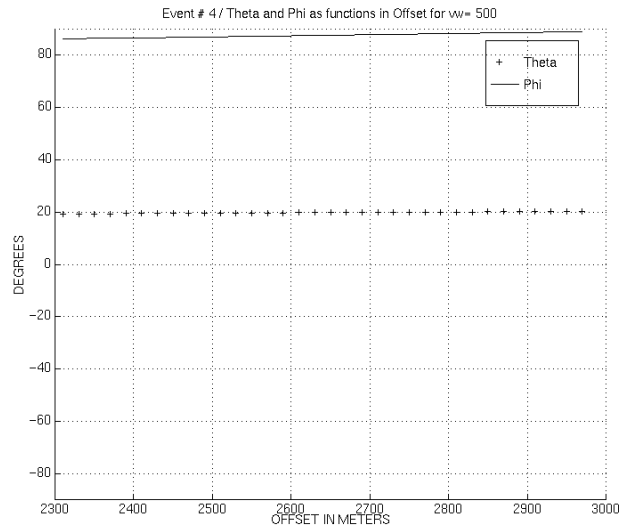


FIG.17. The emergent angle (theta) and displacement angle (phi) as functions of offset.

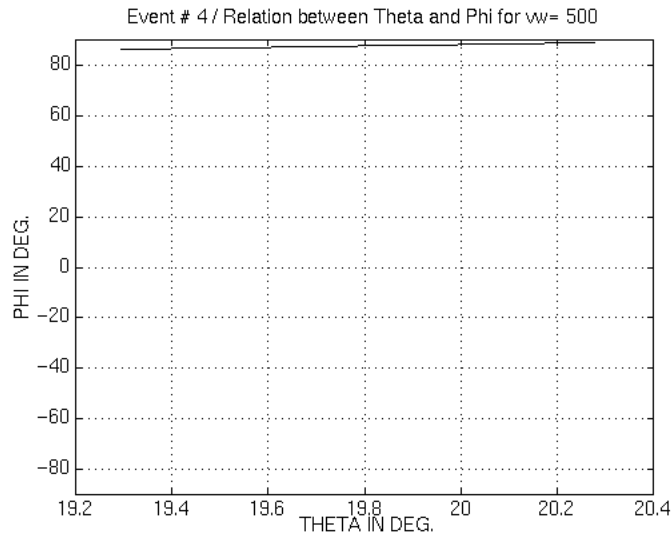


FIG. 18. Relation between theta and phi for event #4.

CONCLUSIONS

The Zoeppritz equations predict a simple relation between the emergence angle and displacement angle for waves recorded at a free surface. P and S waves have distinctly different theta versus phi relationships and there is reason to believe that theta can be distinguished on this basis.

The displacement and emergence angles of real events in raw data can be roughly estimated by picking the events on the component on which they are most visible and fitting low order polynomials to the event's trajectory and amplitudes on all components. The emergence angle estimation requires a value for weathering velocity which is generally not well known.

These measurements are made difficult due to a number of effects such as: interference from other waves, unknown weathering velocities, variations in geophone coupling strength, elevation and near surface changes and so on. Despite such problems, events can be reliably determined as either P or S waves. The results of our analyses strongly suggest that V_p/V_s is at least 5 and perhaps greater in the Blackfoot weathering layer.

ACKNOWLEDGMENTS

We would like to thank Darren Foltinek, Henry Bland and Don Lawton for their help during this process. Also we would like to thank the CREWES Project Sponsors for their assistance.

REFERENCES

- Aki, K, and Richards, P.G., 1980, Quantitative Seismology, Theory and Methods, W.H. Freeman and company.
- Dankbaar, J.W.M., 1985, Separation of P and S waves, Geophysical Prospecting, 33, 970-986.
- Donati and Stewart. Improvement of P-data using 3-C seismic data. The CREWES project. 1994 Research report. Volume 6
- Waters, K.H., 1981, Reflection Seismology, J.H. Wiley.
- Zheng, Ya, 1995, Seismic Polarization filtering: noise reduction and off-line imaging, M.Sc. Thesis, Dept. of Geology and Geophysics, The University of Calgary.